No. 1A-18 $BiFeO_3$, Bismuth ferrite

(M = 312.83)

1a On the basis of X-ray studies of $PbTiO_3$–$BiFeO_3$ solid solutions, it was pointed out that $BiFeO_3$ could have a ferroelectric Curie point at higher temperature [a]). The Curie point was estimated to be about 850 °C from studies of the same solid solution [b]). [a])60Fed [b])61Fed, 62Fed

b

phase	III	II	I
state	(F), A_{magn}	(F), P_{magn}	P, P_{magn}
crystal system	rhombohedral	rhombohedral	(cubic)
space group	$R3c–C_{3v}^6$		
Θ [°C]	370	850	

62Smo, 63Rog, 65Ism, 71Miy

T_{melt} = 930 °C. 65Spe

A structural phase transition occurs close to 1110 K and at 1195 K [c]). [c])93Kub

Further references are available about choice of unit cell: 64Tom, 60Ven, 60Fil, 60Zas

2a Crystal growth: flux method (B_2O_3). 70Tea

Phase diagram of Bi_2O_3–Fe_2O_3: see 64Koi, 65Spe

3a Determination of the atomic structure was done on the single crystal and powder sample by X-ray and neutron diffraction studies. $BiFeO_3$ is rhombohedral with hexagonal lattice. 69Mic, 71Miy, 72Buc

The space group is $R3c–C_{3v}^6$ with two formula units in the unit cell.

Unit cell parameters: rhombohedral, a = 5.616(6) Å, α = 59.35(5)° at RT [a]); hexagonal setting, a_{hex} = 5.5779(3) Å, c_{hex} = 13.8670(5) Å at 25.13 °C [b]). [a])75Jac [b])72Buc, 71Miy, 72Buc

b Ion shifts: Fig. 1A-18-001.
Oxygen shifts in the (111) plane: Fig. 1A-18-002.
Structural parameters: Table 1A-18-001, Table 1A-18-002.
Structural parameters of phase III: Table 1A-18-003, Table 1A-18-004.
X-ray diffraction data and crystal structure at 294 K is reported. See 90Kub, 63Kis, 92Sos

The magnetic structure of $BiFeO_3$ was proved to be G-type by the neutron diffraction experiments: Figs. 1A-18-003, 1A-18-004, 1A-18-005.

4 Unit cell parameters: Figs. 1A-18-006...1A-18-008. See also 66Rog, 64Tom

5a Dielectric constant: Figs. 1A-18-009...1A-18-011.
No reliable data on the dielectric constant in the high temperature region near 850 °C are available.

c	Dielectric hysteresis loops were observed on single crystals grown from a Bi_2O_3 flux. The measured spontaneous polarization was $3.5 \cdot 10^{-2}$ C m^{-2} along the [100] direction, which represents $6.1 \cdot 10^{-2}$ C m^{-2} in the [111] direction. This is considerably lower than expected for a compound with such a high Curie temperature and distortion. The hysteresis loops represent only a partial reversal of the polarization. However, these data serve to confirm the evidence for ferroelectricity in $BiFeO_3$ as required by the space group R3c–C_{3v}^6, found in the atomic structure study.	70Ito, 69Mic, 71Miy
9a	Birefringence: Fig. 1A-18-012. Optical absorption: Fig. 1A-18-013.	
12	Magnetic susceptibility: Fig. 1A-18-014. At RT, no spontaneous magnetic moment was observed in the fields up to 22 kOe. Sublattice magnetization: Fig. 1A-18-015. Magnetoelectric effect: Fig. 1A-18-016, Fig. 1A-18-017; see also	66Yud 85Tab, 93Pop, 85Ish, 75Ism
13c	Mössbauer effect: Figs. 1A-18-018...1A-18-020, Table 1A-18-005. See also The spectrum consists of two superimposed six-line spectra; H_{int} = 39.6, 39.8·10^6 A m^{-1} (498, 561 kOe). See also	76DeS 76DeS 65Mit, 71Bir
15	Domain structure: see	93Kub, 95Kub

Table 1A-18-001. $BiFeO_3$. Fractional atomic coordinates, temperature parameters and lattice parameters obtained by neutron powder profile analysis [75Jac]. *R*: discrepancy factors, *B*: temperature parameters defined by Eq. (e) in Introduction.

(a) 4.2 K

Atom	Position	*x*	*y*	*z*	*B* [Å^2]
Fe	2(a)	0.0	0.0	0.0	0.10(8)
Bi	2(a)	0.2802(3)	0.2802(3)	0.2802(3)	0.13(8)
O	6(b)	–0.3248(7)	0.8044(7)	0.2130(9)	0.33(6)
a = 5.617(3) Å	α = 59.40(5)°	gS = 4.09(3)			
R(profile) = 7.0 %	R(expected) = 3.1 %				
R(intensities)$_{nuclear}$ = 2.6 %	R(intensities)$_{magn}$ = 8.1 %				

(b) Room temperature

Atom	Position	*x*	*y*	*z*
Fe	2(a)	0.0	0.0	0.0
Bi	2(a)	0.2797(4)	0.2797(4)	0.2797(4)
O	6(b)	–0.3243(15)	0.8026(16)	0.2146(16)
a = 5.616(6) Å	α = 59.35(5)°	gS = 3.86(4)		
R(profile) = 8.0 %	R(expected) = 4.4 %			
R(intensities)$_{nuclear}$ = 3.1 %	R(intensities)$_{magn}$ = 5.8%			

Table 1A-18-002. $BiFeO_3$. Interatomic distances and angles [75Jac].

(a) 4.2 K			
Distance	[Å]	Distance	[Å]
Fe–O	1.945(3)	O–O	2.997(4)
	2.109(4)		2.854(6)
			2.816(6)
Bi–O	3.450(6)		2.706(4)
	3.217(3)		
	2.519(3)	Bi–Fe	3.872(3)
	2.252(6)		3.038(3)
Angle	[°]		
O–Fe–O	100.8(2)		
	89.4(2)		
	87.9(2)		
	79.8(2)		

(b) Room temperature			
Distance	[Å]	Distance	[Å]
Fe–O	1.95(1)	O–O	3.00(1)
	2.12(1)		2.73(1)
			2.86(1)
Bi–O	3.45(1)		2.83(1)
	3.22(1)		
	2.53(1)	Bi–Fe	3.88(1)
	2.27(1)		3.06(1)
Angle	[°]		
O–Fe–O	100.7(4)		
	89.3(4)		
	88.0(4)		
	80.1(4)		

Table 1A-18-003. $BiFeO_3$. Symbols to describe atomic coordinates in the hexagonal cell (R3c) to be used in Table 1A-18-004 [75Meg].

Atom	*x*	*y*	*z*
A	0	0	$z_A = 1/4 + s$
B	0	0	$z_B = t$
O	$\underbrace{\frac{1}{6} - 2e - 2d}_{x_O}$	$\underbrace{\frac{1}{3} - 4d}_{y_O}$	1/12

Table 1A-18-004. $BiFeO_3$. Structural parameters refined by profile analysis of neutron diffraction [80Fis]. See Table 1A-18-003. ω : tilt angle related to e by tan $\omega = 4\sqrt{3}\,e$, ξ : octahedron strain, compression or elongation along the triad axis. μ: magnetic moment.

T [K]	4.2	77	293	513
a_{hex} [Å]	5.577(7)	5.578(7)	5.585(7)	5.593(7)
c_{hex} [Å]	13.850(18)	13.855(18)	13.884(18)	13.917(18)
z_{Bi}	0.2989(5)	0.2993(6)	0.2987(5)	0.2972(5)
z_{Fe}	0.0198(6)	0.0203(6)	0.0196(5)	0.0186(5)
x_O	0.2398(8)	0.2398(8)	0.2379(8)	0.2370(6)
y_O	0.3518(13)	0.3514(13)	0.3506(12)	0.3502(11)
s	0.0489(5)	0.0493(6)	0.0487(5)	0.0472(5)
t	0.0198(6)	0.0203(6)	0.0196(5)	0.0186(5)
d	–0.0046(3)	–0.0045(3)	–0.0043(3)	–0.0042(3)
e	–0.0319(5)	–0.0316(5)	–0.0313(5)	–0.0310(4)
$\|\omega\|$ [°]	12.5(2)	12.3(2)	12.2(2)	12.1(2)
ζ	–0.0102(8)	–0.0095(8)	–0.0082(7)	–0.0068(6)
B [Å^2]	0.07(9)	0.27(9)	0.56(9)	0.82(8)
$\mu = gS$ [μ_B]	4.33(4)	4.35(5)	4.00(4)	2.53(4)
R_{prof}	8.4	8.8	8.4	7.7
R_{nucl}	1.7	2.0	1.7	1.9
R_{magn}	6.4	7.0	7.8	9.2

T [K]	604	683	878
a_{hex} [Å]	5.598(7)	5.582(7)	5.621(7)
c_{hex} [Å]	13.937(18)	13.900(18)	13.980(18)
z_{Bi}	0.2972(5)	0.2974(5)	0.2950(6)
z_{Fe}	0.0188(5)	0.0193(6)	0.0178(7)
x_O	0.2360(7)	0.2353(12)	0.2338(8)
y_O	0.3503(11)	0.3534(9)	0.3513(12)
s	0.0472(5)	0.0474(5)	0.0450(6)
t	0.0188(5)	0.0193(6)	0.0178(6)
d	–0.0042(3)	–0.0050(2)	–0.0045(3)
e	–0.0304(4)	–0.0293(5)	–0.0291(5)
$\|\omega\|$ [°]	11.9(2)	11.5(2)	11.4(2)
ζ	–0.0039(6)	–0.0081(6)	–0.0036(7)
B [Å^2]	0.78(8)	1.09(7)	1.8(1)
$\mu = gS$ [μ_B]	–	–	–
R_{prof}	7.7	10.0	8.8
R_{nucl}	2.5	5.0	3.0
R_{magn}	–	–	–

Table 1A-18-005. $BiFeO_3$. D and β in the relation $H_{int}(T)/H_{int}(0) = D(1-T/\theta_N)^{\beta}$ [75Jac].

Temperature region	D	β
$0.01 < 1-T/\Theta_N < 0.1$	1.24(5)	0.37(2)
$0.1 < 1-T/\Theta_N < 0.5$	1.12(3)	0.33(2)

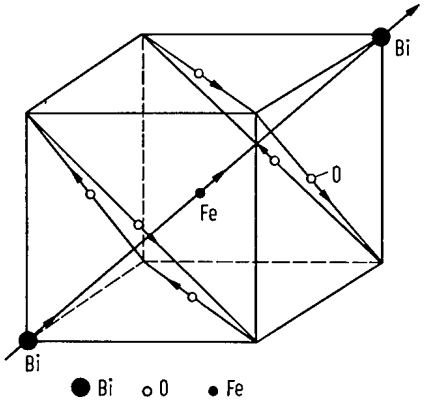

Fig. 1A-18-001. $BiFeO_3$. Ion shifts [69Mic]. The framework shown here does not correspond to the rhombohedral cell containing two formula units of $BiFeO_3$, but to one half of it. Magnitude of ion shifts: Bi: 0.62 Å along [111], Fe: 0.23 Å along [111], O: 0.30 Å rotating about [111]. Errors in all values: ± 0.03 Å.

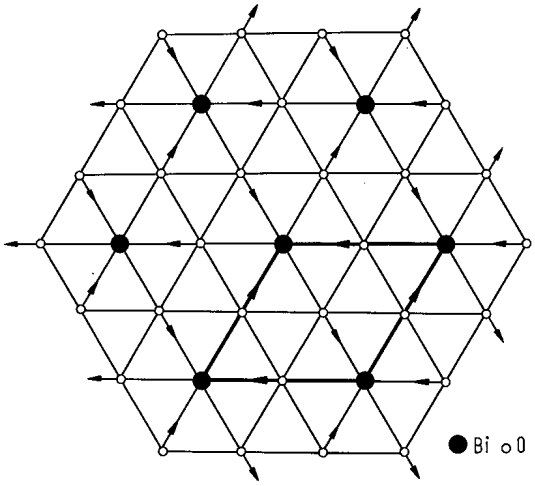

Fig. 1A-18-002. $BiFeO_3$. Oxygen shifts from ideal perovskite positions in the (111) plane [69Mic]. Bi is shifted normal to the plane. $BiFeO_3$ may also be represented by a hexagonal unit cell whose base is heavily drawn, and which contains six formula units of $BiFeO_3$.

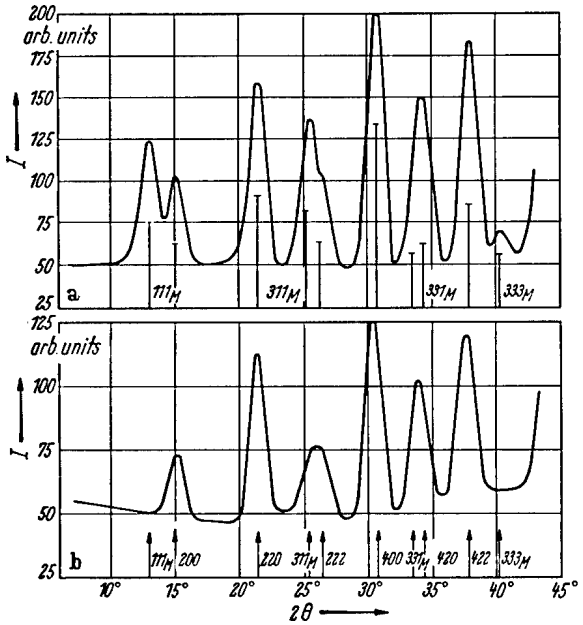

Fig. 1A-18-003. $BiFeO_3$. Neutron diffraction patterns [63Kis]. (**a**) 20 °C, (**b**) 520 °C. *I*: intensity; *M*: magnetic scattering maximum.

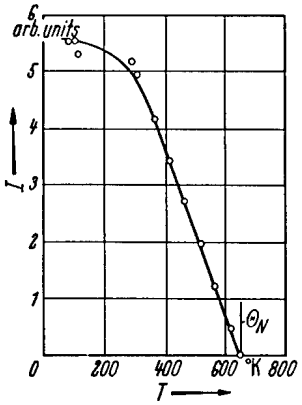

Fig. 1A-18-004. $BiFeO_3$. *I* vs. *T* [63Kis]. *I*: intensity of the (111) magnetic maximum. See Fig. 1A-18-003.

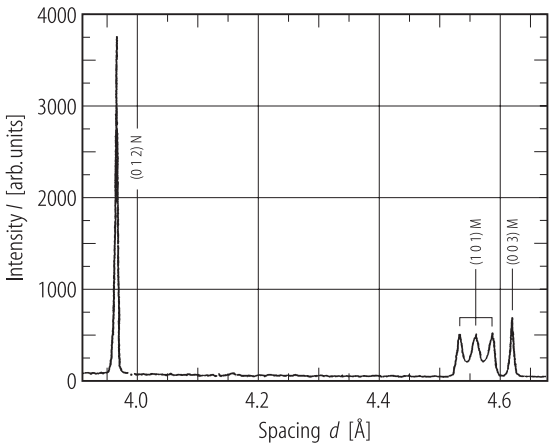

Fig. 1A-18-005. $BiFeO_3$. Time-of-flight neutron diffraction pattern [92Sos].

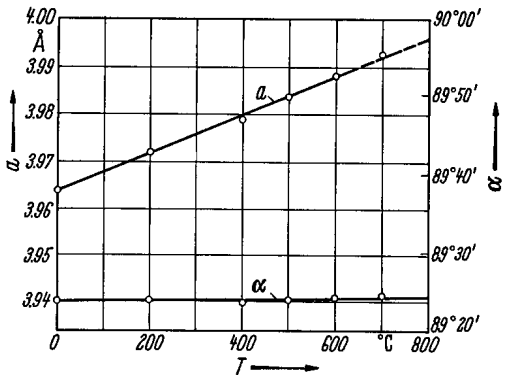

Fig. 1A-18-006. $BiFeO_3$. a, α vs. T [61Fed].

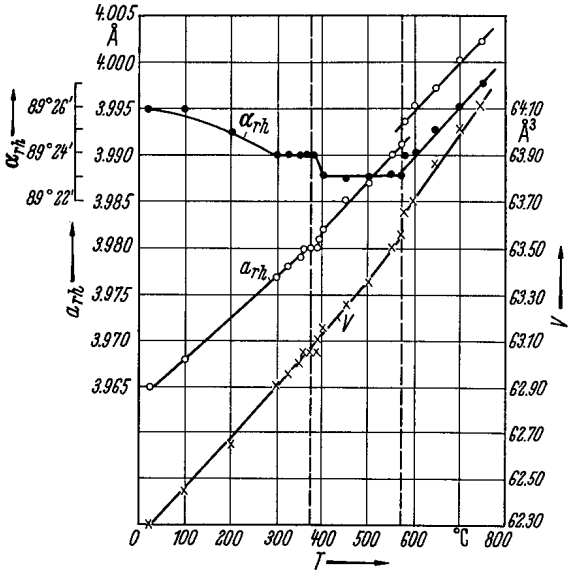

Fig. 1A-18-007. $BiFeO_3$. a_{rh}, α_{rh}, V vs. T [65Ism].

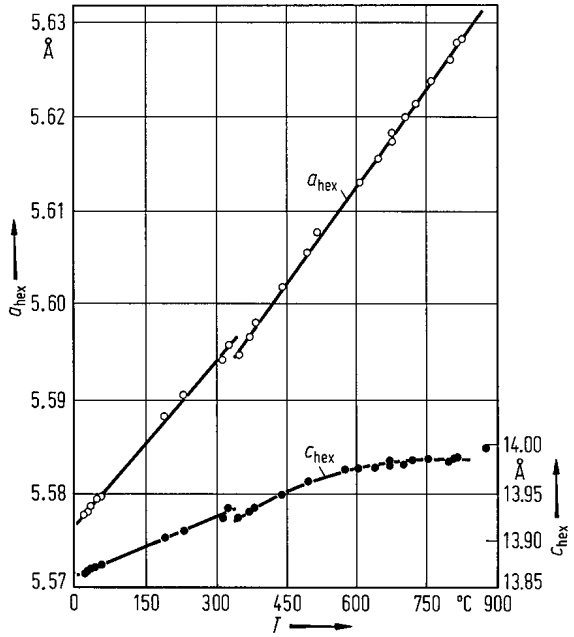

Fig. 1A-18-008. $BiFeO_3$. a_{hex}, c_{hex} vs. T [72Buc].

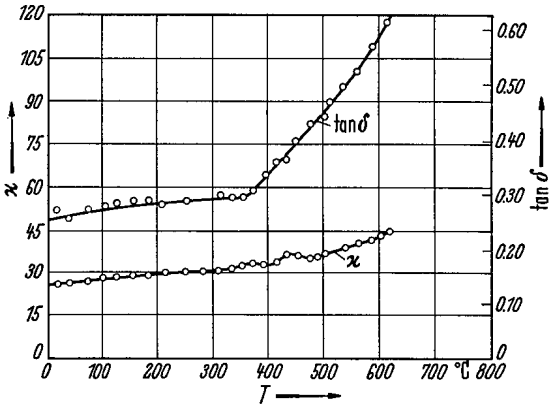

Fig. 1A-18-009. $BiFeO_3$. κ, $\tan\delta$ vs. T [66Rog].

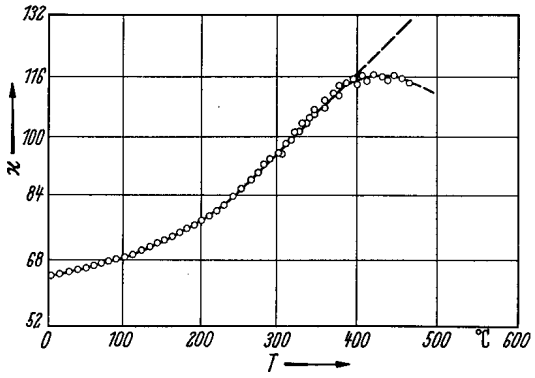

Fig. 1A-18-010. $BiFeO_3$. κ vs. T [64Tom].

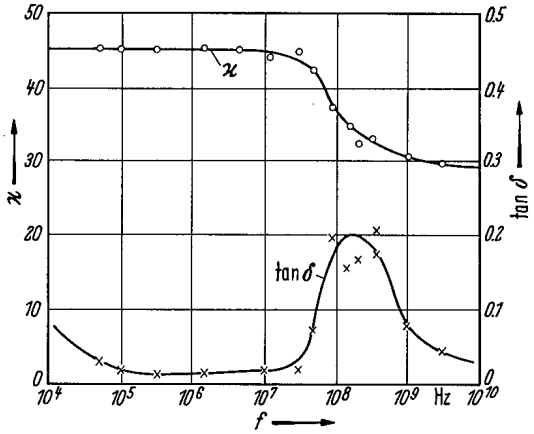

Fig. 1A-18-011. $BiFeO_3$. κ, $\tan\delta$ vs. f [66Rog].

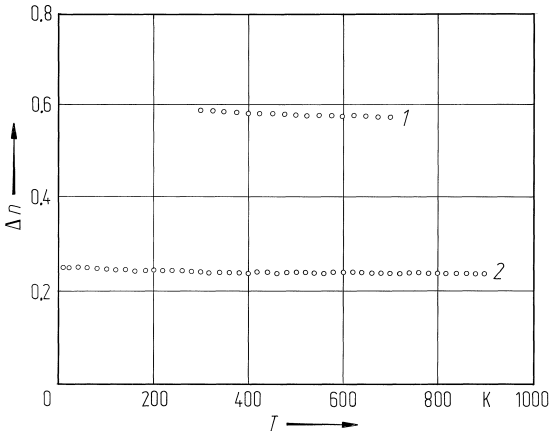

Fig. 1A-18-012. $BiFeO_3$. Δn vs. T [84Tab]. Curve *1*: $n_\gamma - n_\alpha$, λ = 644 nm; *2*: $n_\gamma - n'_\alpha$ (birefringence measured on (110) plate. Optical axis inclined at 54.74" to the surface of the (110) plate), λ = 546 nm.

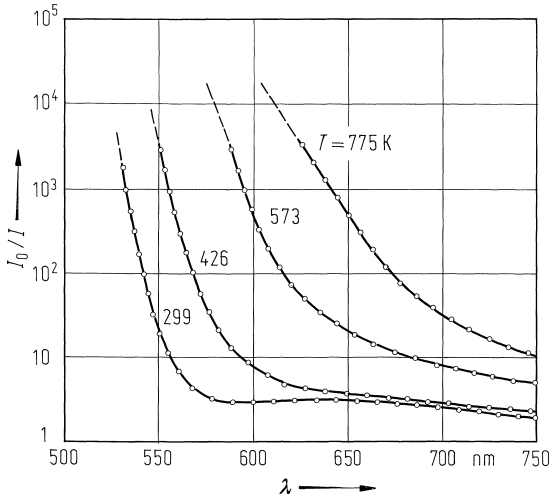

Fig. 1A-18-013. $BiFeO_3$. Optical absorption I_0 / I vs. λ [84Tab]. Parameter: T. Thickness: 8 µm.

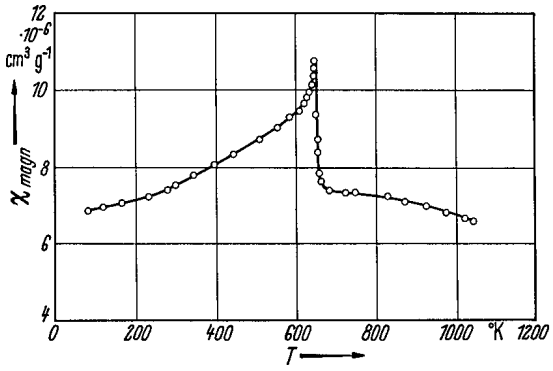

Fig. 1A-18-014. $BiFeO_3$. χ_{magn} vs. T [66Yud].

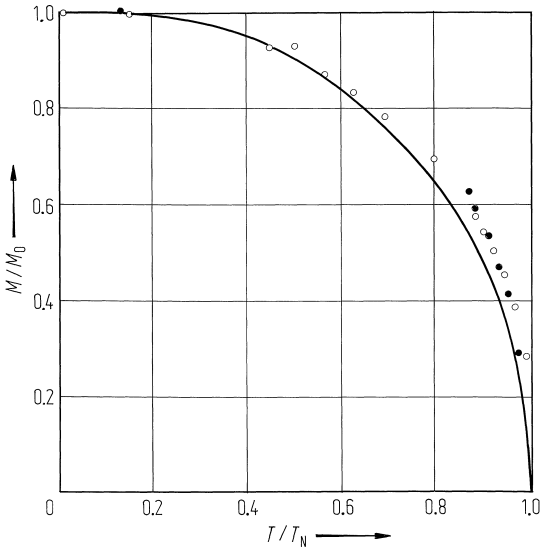

Fig. 1A-18-015. $BiFeO_3$. M/M_0 vs. T/T_N [80Fis]. M/M_0: reduced sublattice magnetization, T_N = 595(15) K. Full circles: neutron diffraction [80Fis], open circles: Mössbauer effect [73Bla]. The curve shows Brillouin function for S = 5/2.

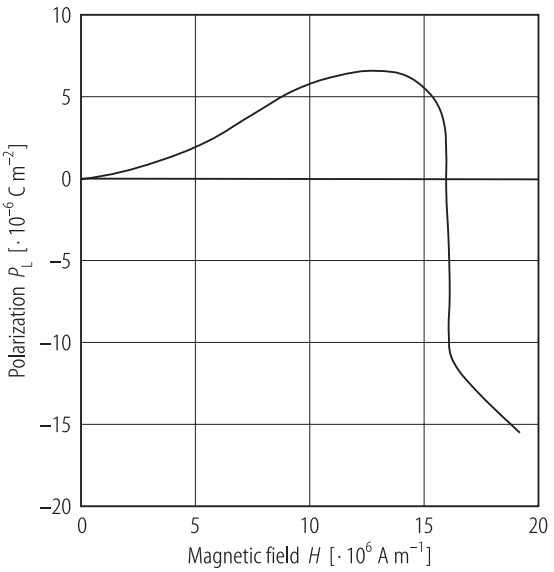

Fig. 1A-18-016. $BiFeO_3$. P_L vs. H [93Pop]. P_L: longitudinal polarization.

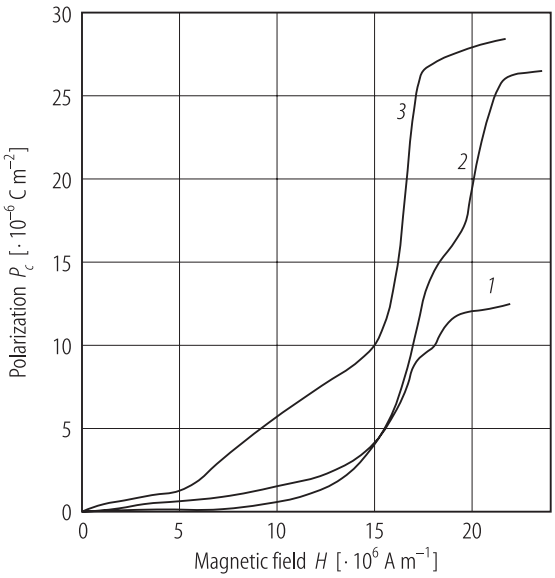

Fig. 1A-18-017. $BiFeO_3$. P_c vs. H [93Pop]. P_c: c-axis polarization. Curve *1*: $H \parallel a$, *2*: $H \parallel b$, *3*: $H \parallel c$.

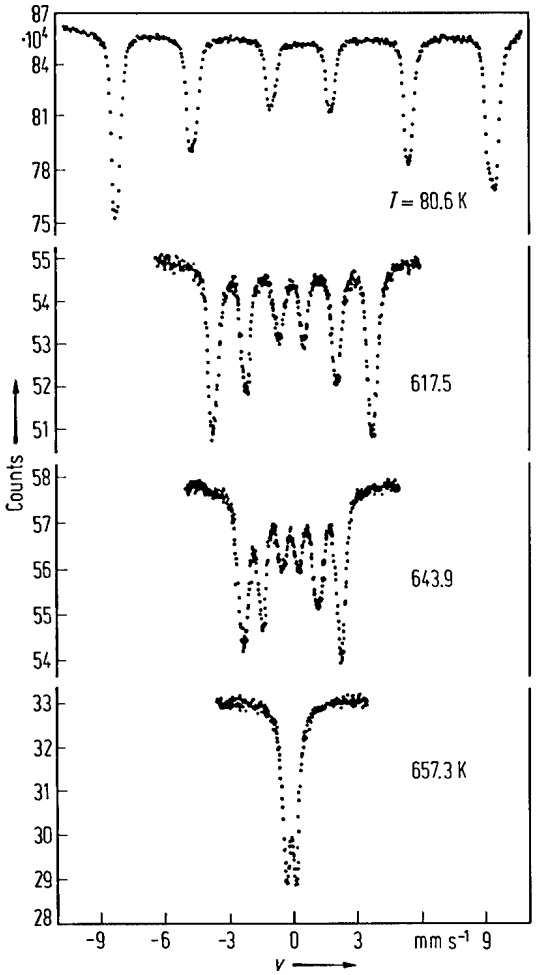

Fig. 1A-18-018. $BiFeO_3$. (^{57}Co) Mössbauer resonance absorption spectra at different temperatures [65Mit]. N/N_0: counting ratio, v: velocity of absorber.

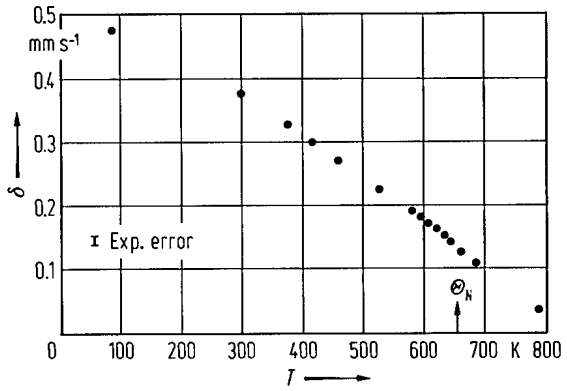

Fig. 1A-18-019. $BiFeO_3$. δ vs. T [71Bir]. δ: isomer shift. The values are relative to nitro-prusside standard.

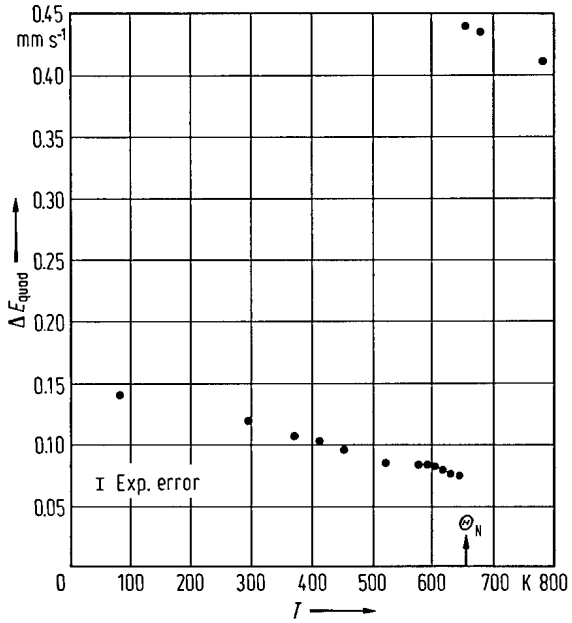

Fig. 1A-18-020. $BiFeO_3$. ΔE_{quad} vs. T [71Bir]. ΔE_{quad}: quadrupole splitting.

References

60Fed Fedulov, S.A., Venevtsev, Yu.N., Zhdanov, G.S., Smazhevskaya, E.G., Rez, I.S.: Thesis of Reports of the Third All-Union Conference on Ferroelectricity, Izd.-vo AN SSSR, 1960, p. 51 (in Russian).

60Fil Filip'ev, V.S., Smolyaninov, N.P., Fesenko, E.G., Belyaev, I.N.: Kristallografiya **5** (1960) 958; Sov. Phys. Crystallogr. (English Transl.) **5** (1961) 913.

60Ven Venevtsev, Yu.N., Zhdanov, G.S., Solov'ev, S.P., Bezus, E.V., Ivanova, V.V., Fedulov, S.A., Kapyshev, A.G.: Kristallografiya **5** (1960) 620; Sov. Phys. Crystallogr. (English Transl.) **5** (1961) 694.

60Zas Zaslavskii, A.I., Tutov, A.G.: Dokl. Akad. Nauk SSSR **135** (1960) 815; Sov. Phys. Dokl. (English Transl.) **5** (1961)1257.

61Fed Fedulov, S.A.: Dokl. Akad. Nauk SSSR **139** (1961) 1345; Sov. Phys. Dokl. (English Transl.) **6** (1962) 729.

62Fed Fedulov, S.A., Venevtsev, Yu.N., Zhdanov, G.S., Smazhevskaya, E.G., Rez, I.S.: Kristallografiya **7** (1962) 77; Sov. Phys. Crystallogr. (English Transl.) **7** (1962) 62.

62Smo Smolenskii, G.A., Yudin, V.M., Sher, E.S., Stolypin, Yu.E.: Zh. Eksp. Teor. Fiz. **43** (1962) 877; Sov. Phys. JETP (English Transl.) **16** (1963) 622.

63Kis Kiselev, S.V., Kshnyakina, A.N., Ozerov, R.P., Zhdanov, G.S.: Fiz. Tverd. Tela **5** (1963) 3312; Sov. Phys. Solid State (English Transl.) **5** (1964) 2425.

63Rog Roginskaya, Yu.E., Venevtsev, Yu.N., Fedulov, S.A., Zhdanov, G.S.: Kristallografiya **8** (1963) 610; Sov. Phys. Crystallogr. (English Transl.) **8** (1964) 490.

64Koi Koizumi, H., Niizeki, N., Ikeda, T.: Jpn. J. Appl. Phys. **3** (1964) 495.

64Tom Tomashpol'skii, Yu.Ya., Venevtsev, Yu.N., Zhdanov, G.S.: Zh. Eksp.Teor. Fiz. **46** (1964) 1921; Sov. Phys. JETP (English Transl.) **19** (1964) 1294.

65Ism Ismailzade, I.G.: Bull. Acad. Sci. USSR, Phys. Ser. (English Transl.) **29** (1965) 1032.

65Mit Mitrofanov, K.P., Viskov, A.S., Plotnikova, M.V., Venevtsev, Yu.N., Shpinel', V.S.: Izv. Akad. Nauk SSSR, Ser. Fiz. **29** (1965) 2029; Bull. Acad. Sci. USSR, Phys. Ser. (English Transl.) **29** (1965)1865.

65Spe Speranskaya, E.I., Skorikov, V.M., Rode, E.Ya., Terekhova, V.A.: Izv. Akad. Nauk SSSR, Ser. Khim. **5** (1965) 905; Bull. Acad. Sci. USSR, Div. Chem. Sci. (English Transl.) **5** (1965) 874.

66Rog Roginskaya, Yu.E., Tomashpol'skii, Yu.Ya., Venevtsev, Yu.N., Petrov, V.M., Zhdanov, G.S.: Zh. Eksp. Teor. Fiz. **50** (1966) 69; Sov. Phys. JETP (English Transl.) **23** (1966) 47.

66Yud Yudin, V.M.: Fiz. Tverd. Tela **8** (1966) 267; Sov. Phys. Solid State (English Transl.) **8** (1966) 217.

67Tom Tomashpol'skii, Yu.Ya., Venevtsev, Yu.N.: Kristallografiya **12** (1967) 24; Sov. Phys. Crystallogr. (English Transl.) **12** (1967)18.

69Mic Michel, C., Moreau, J.-M., Achenbach, G.D., Gerson, R., James, W.J.: Solid State Commun. **7** (1969) 701.

70Ito Itoh, Y., Miyazawa, S., Yamada, T., Iwasaki, H.: Jpn. J. Appl. Phys. **9** (1970) 157.

70Tea Teague, J.R., Gerson, R., James, W.J.: Solid State Commun. **8** (1970) 1073.

71Bir Biran, A., Montano, P.A., Shimony, U.: J. Phys. Chem. Solids **32** (1971) 327.

71Miy Miyazawa, S., Iwasaki, H.: J. Cryst. Growth **10** (1971) 276.

72Buc Bucci, J.D., Robertson, B.K., James, W.J.: J. Appl. Cryst. **5** (1972) 187.

73Bla Blaauw, C., Van der Woude, F.: J. Phys. C **6** (1973) 1422.

75Ism Ismailzade, I.H., Yakupov, R.G.: Phys. Status Solidi (a) **32** (1975) K161.

75Jac Jacobson, A.J., Fender, B.E.F.: J. Phys. C **8** (1975) 844.

75Meg Megaw, H.D., Darlington, C.N.W.: Acta Crystallogr., Sect. A **31** (1975) 161.

76DeS De Sitter, J., Dauwe, C., De Grave, E., Govaert, A.: Solid State Commun. **18** (1976) 645.

80Fis Fischer, P., Polomska, M., Sosnowska, I., Szymanski, M.: J. Phys. C **13** (1980) 1931.

84Tab Tabares-Munoz, C., Rivera, J.-P., Schmid, H.: Ferroelectrics **55** (1984) 235.
85Ish Ishikawa, K., Tomoda, W., Takeuchi, K., Toyoda, K.: J. Cryst. Growth **71** (1985) 232.
85Tab Tabares-Munoz, C., Rivera, J.-P., Bezinges, A., Monnier, A., Schmid, H.: Jpn. J. Appl. Phys. **24** (1985), Suppl. 24–2, 1051.
90Kub Kubel, F ., Schmid, H.: Acta Crystallogr., Sect. B **46** (1990) 698.
92Sos Sosnowska, I., Loewenhaupt, M., David, W.I.F., Ibberson, R.M.: Physica B **180**–**181** (1992) 117.
93Kub Kubel, F., Schmid, H.: J. Cryst. Growth **129** (1993) 515.
93Pop Popov, Y.F., Zvezdin, A.K., Vorob'ed, G.P., Kadomtseva, A.M., Murashev, V.A., Rakov, D.N.: JETP Lett. (English Transl.) **57** (1993) 69.
95Kub Kubel, F.: Z. Kristallogr. **210** (1995) 5.